Supporting Information

Stepwise Engineering Pore Environment and Enhancing CO_2/R22 Adsorption Capacity through Dynamic Spacer Installation and Functionality Modification

Cheng-Xia Chen, Qian-Feng Qiu, Chen-Chen Cao, Mei Pan, Hai-Ping Wang, Ji-Jun Jiang, Zhang-Wen Wei*, Kelong Zhu, Guangqin Li and Cheng-Yong Su*

MOE Laboratory of Bioinorganic and Synthetic Chemistry, Lehn Institute of Functional materials, School of Chemistry, Sun Yat-Sen University, Guangzhou 510275, China.

Email: weizhw3@mail.sysu.edu.cn; cesscy@mail.sysu.edu.cn

S1. Materials and Instrumentation

All the reagents and solvents were purchased from commercial sources and directly utilized without further purification. Solid-state IR spectra were recorded using Nicolet/Nexus-670 FT-IR spectrometer in the region of 4000-400 cm^{-1} using KBr pellets. Single crystal X-ray diffraction data were collected on an Agilent Technologies SuperNova X-RAY diffractometer system equipped with a Cu sealed tube (λ = 1.54178) at 50 kV and 0.80 mA. Powder X-ray diffraction (PXRD) was carried out with a RigakuSmartLab diffractometer (Bragg-Brentano geometry, Cu Kα1 radiation, λ = 1.54056 Å). Thermogravimetric analyses (TGA) were performed on a NETZSCH TG209 system in nitrogen and under 1 atm of pressure at a heating rate of 10 °C min^{-1}. Nuclear magnetic resonance (NMR) data were collected on a 400 MHz Nuclear Magnetic Resonance Spectrometer. Gas adsorption isotherms for pressures in the range of 0-1.0 bar were obtained by a volumetric method using a quantachrome autosorb-iQ2-MP gas adsorption analyzer. Gas adsorption measurements were performed using ultra-high purity N_2, CH_4, CO_2 and R22 gases.

S2. Ligand Synthesis

2,2'-dimethylbiphenyl-4,4'-dicarboxylic acid (**H_2L^1**),[1] 2'-(azidomethyl)-[1,1':4',1"-terphenyl]-4,4"-dicarboxylic acid (**H_2L^2**),[2] 2',5'-bis(azidomethyl)-[1,1':4',1"-terphenyl]-4,4"-dicarboxylic acid (**H_2L^3**),[2] and 2',3',5',6'-tetrakis(azidomethyl)-[1,1':4',1"-terphenyl]-4,4"-dicarboxylic acid (**H_2L^4**)[2] were synthesised and characterised based on literature procedures.

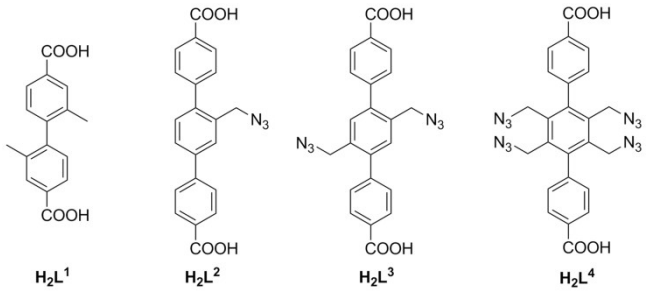

Scheme S1 The structures of ligands.

S3. MOF Synthesis

3.1 Synthesis of PCN-700-o and PCN-700-c

PCN-700 and PCN-700-c were prepared using a modified literature procedure.[1]

3.2 Synthesis of LIFM-90

PCN-700-o (10 mg), $\mathbf{H_2L^1}$ (1.7 mg), $\mathbf{H_2L^2}$ (2.4 mg) and DMF (2.0 mL) were charged in a vial. The mixture was heated in a 85 ºC oven for 40 h. The crystals were washed with DMF (3×), soaked in DMF (5 mL) at 85 ºC for 24 h, and finally washed with DMF again (3×) (11.3 mg, yield: 89.0 %). FTIR (KBr): ν= 2941 (w), 2097 (m), 1591 (s), 1547 (s), 1414 (s), 1334 (s), 1208 (w), 1140 (w), 1023 (s), 847 (s), 773 (s), 681 (w), 655 (s) cm^{-1}.

3.3 Synthesis of LIFM-91

Propargylamine (50 uL) were added to a mixture of LIFM-90 (100 mg) and CuI (3.0 mg) in DMF (2.0 ml) in 5 mL round-bottom flask. The reaction mixture was stirred at 60 °C for 30 h. The resulting precipitate was collected by centrifugation, washing with DMF, metanol, and drying to afford brown solid in quantitative yield. FTIR (KBr): ν= 3306 (w), 2941 (w), 1593 (m), 1548 (m), 1415 (s), 1384 (s), 1208 (w), 1140 (w), 1024 (s), 908 (w), 779 (s), 656 (s) cm^{-1}.

3.4 Synthesis of LIFM-92

PCN-700-o (10 mg), $\mathbf{H_2L^1}$ (1.7 mg), $\mathbf{H_2L^3}$ (2.7 mg) and DMF (2.0 mL) were charged in a vial. The mixture was heated in a 85 ºC oven for 40 h. The crystals were washed with DMF (3×), soaked in DMF (5 mL) at 85 ºC for 24 h, and finally washed with DMF again (3×) (12.3 mg, yield: 97.6 %). FTIR (KBr): ν= 3313 (w), 2095 (m), 1589 (m), 1545 (m), 1414 (s), 1384 (s), 1207 (w), 1140 (w), 1007 (m), 908 (w), 849 (w), 778 (s), 654 (s) cm^{-1}.

3.5 Synthesis of LIFM-93

Propargylamine (100 uL) were added to a mixture of LIFM-92 (100 mg) and CuI (3.0 mg) in DMF (2.0 ml) in 5 mL round-bottom flask. The reaction mixture was stirred at 60 °C for 30 h. The resulting precipitate was collected by centrifugation, washing with DMF, metanol, and drying to afford brown solid in quantitative yield.

FTIR (KBr): ν= 3305 (m), 2942 (w), 2830 (w), 1591 (m), 1547 (m), 1412 (s), 1384 (s), 1208 (w), 1119 (w), 1022 (s), 779 (m), 654 (s) cm^{-1}.

3.6 Synthesis of LIFM-94

PCN-700-o (10 mg), $\mathbf{H_2L^1}$ (1.7 mg), $\mathbf{H_2L^4}$ (3.4 mg) and DMF (2.0 mL) were charged in a vial. The mixture was heated in a 85 ºC oven for 40 h. The crystals were washed with DMF (3×), soaked in DMF (5 mL) at 85 ºC for 24 h, and finally washed with DMF again (3×) (12.8 mg, yield: 94.1 %). FTIR (KBr): ν= 2941 (w), 2092 (m), 1590 (m), 1547 (m), 1414 (s), 1385 (s), 1207 (w), 1141 (w), 1022 (s), 908 (w), 849 (w), 775(s), 681 (m), 655 (s) cm^{-1}.

3.7 Synthesis of LIFM-95

Propargylamine (190 uL) were added to a mixture of LIFM-94 (100 mg) and CuI (3.0 mg) in DMF (2.0 ml) in 5 mL round-bottom flask. The reaction mixture was stirred at 60 °C for 30 h. The resulting precipitate was collected by centrifugation, washing with DMF, metanol, and drying to afford brown solid in quantitative yield. FTIR (KBr): ν= 3281 (w), 2943 (w), 2867 (m), 1593 (m), 1546 (m), 1412 (s), 1382 (s), 1208 (w), 1140 (w), 1022 (s), 777 (s), 653 (s) cm^{-1}.

S4. Single Crystal X-Ray Crystallography

Single crystal of LIFM-90, LIFM-92 and LIFM-94 were carefully picked and coated in paratone oil, attached to a glass silk which was inserted into a stainless steel stick, then quickly transferred to the Agilent Gemini S Ultra CCD Diffractometer with the Enhance X-ray Source of Cu radiation (λ = 1.54178 Å) using the ω-ϕ scan technique. All of the structures were solved by direct methods and refined by full-matrix least squares against F^2 using the SHELXL programs.[3] Hydrogen atoms were placed in geometrically calculated positions and included in the refinement process using riding model with isotropic thermal parameters: Uiso(H) = 1.2 Ueq(-CH). All the electrons of disordered solvent molecules which cannot be determined, are removed by SQUEEZE routine of PLATON program.[4] Crystal and refinement parameters are listed in Table S1.

Table S1 Crystallographic data for LIFM-90, LIFM-92 and LIFM-94

Compound	**LIFM-90**	**LIFM-92**	**LIFM-94**
CCDC No.	1544323	1544324	1544325
Formula	$C_{101}H_{73}N_3O_{32}Zr_6$	$C_{102}H_{74}N_6O_{32}Zr_6$	$C_{104}H_{76}N_{12}O_{34}Zr_6$
Formula Weight	2387.94	2442.99	2585.08
Shape / Color	Block / Colorless	Block/ Colorless	Block/ Colorless
Crystal System	Tetragonal	Tetragonal	Tetragonal
Space Group	$P4_2/mmc$	$P4_2/mmc$	$P4_2/mmc$
T (K)	173(2)	173(2)	173(2)
a (Å)	23.0842(1)	23.1092(10)	23.0742(4)
b (Å)	23.0842(1)	23.1092(10)	23.0742(4)
c (Å)	18.7738(2)	18.795(3)	18.6187(8)
α / β / γ (°)	90.0 / 90 / 90	90.0 / 90 / 90	90.0 / 90 / 90
V (Å^3)	10004.19(14)	10037.57(18)	9912.9(5)
Z	2	2	2
D_{calc} (g/cm^3)	0.793	0.808	0.866
μ (mm^{-1})	2.822	2.825	2.897
F (000)	2392	2448	2592
R_{int}	0.0275	0.0320	0.0538
Reflections collected / unique	18268 / 4546	19865 / 4585	19426 / 4560
Completeness to theta	97.7 %	98.3 %	98.4 %
Data / Restraints / parameters	4546 / 337 / 282	4585 / 291 / 222	4560 / 475 / 302
R_1 [I>2σ(I)]	0.0603	0.0581	0.0926
wR_2 [I>2σ(I)]	0.1943	0.1892	0.2422
R_1 (all data)	0.0644	0.0674	0.1265
wR_2 (all data)	0.1996	0.2037	0.2878
GOF	1.063	1.133	1.059

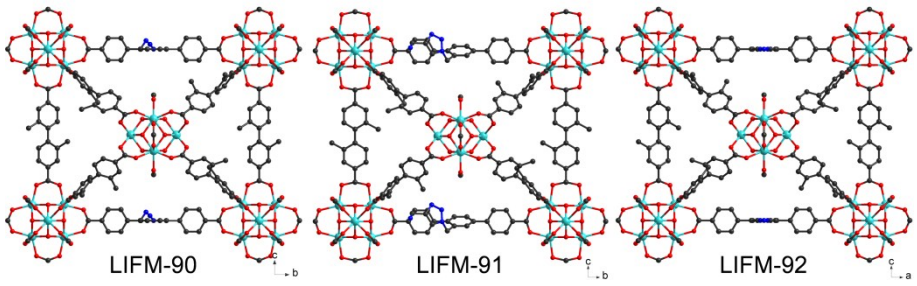

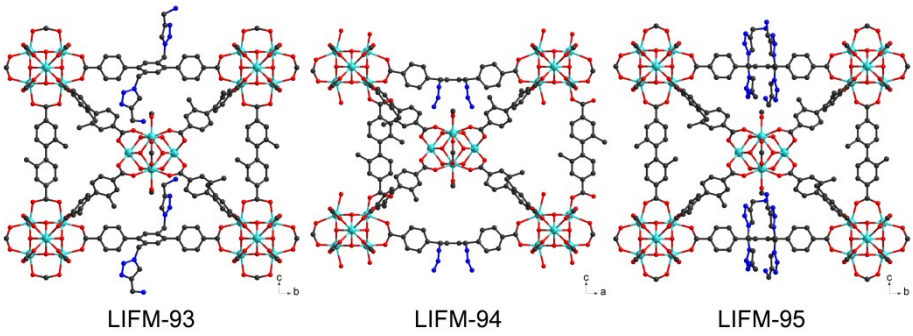

Fig. S1 Presenting the installed spacers in LIFM-90—95. Color scheme: grey, C; red, O; aqua, Zr; blue, N. All hydrogen atoms are omitted for clarity (Strucutres of LIFM-91, LIFM-93 and LIFM-95 are obtained from a simple simulation with Materials Studio 6.1 and only used for general presentation.[5])

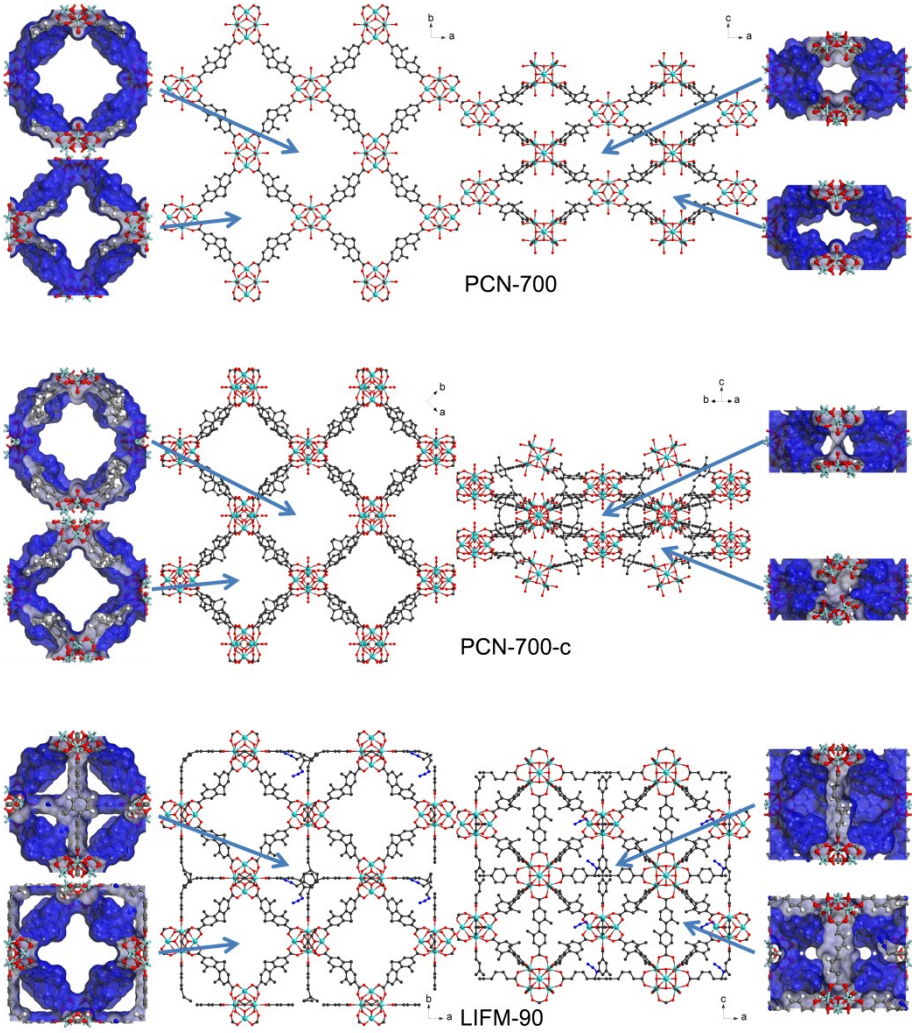

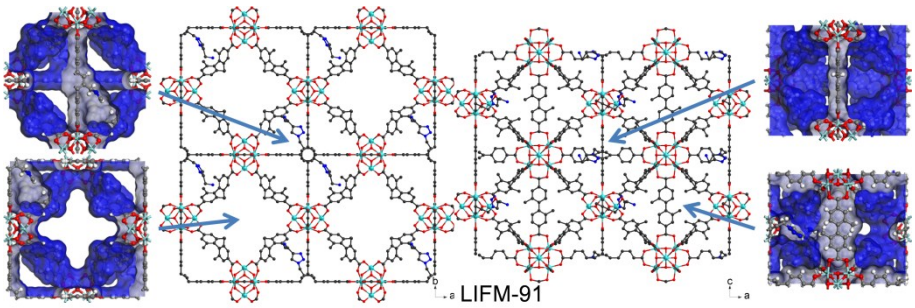
LIFM-91

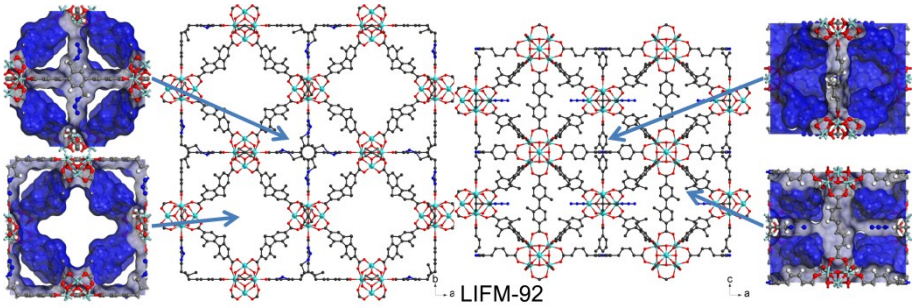
LIFM-92

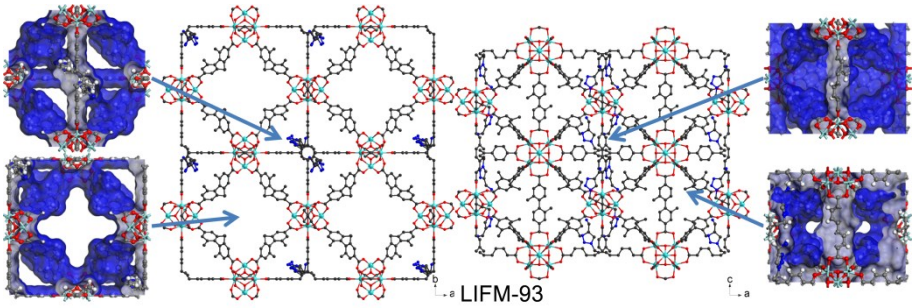
LIFM-93

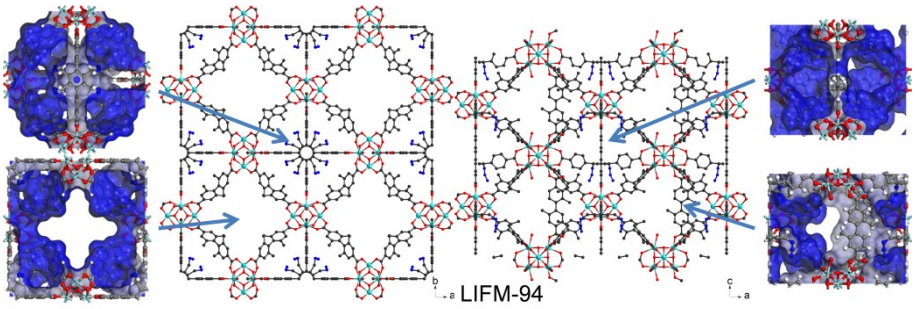
LIFM-94

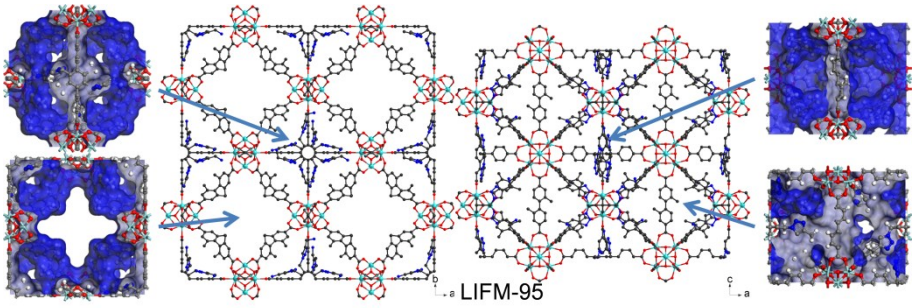
LIFM-95

Fig. S2 Presenting the channels along c-axis and a-/b-axis in PCN-700 and LIFM-90—95. (Strucutres of LIFM-91, LIFM-93 and LIFM-95 are obtained from a simple simulation with Materials Studio 6.1 and only used for general presentation.[5])

S5. Powder X-ray Diffraction

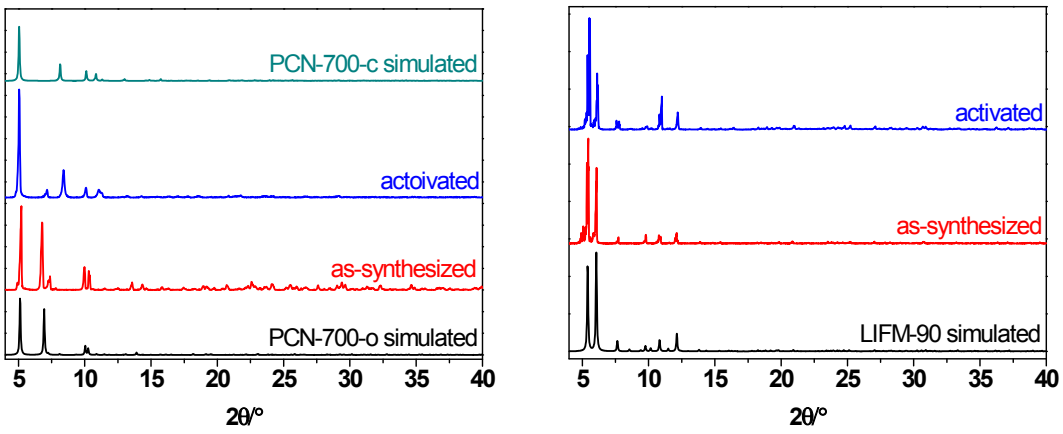

Fig. S3 PXRD patterns of PCN-700 (left) and LIFM-90 (right).

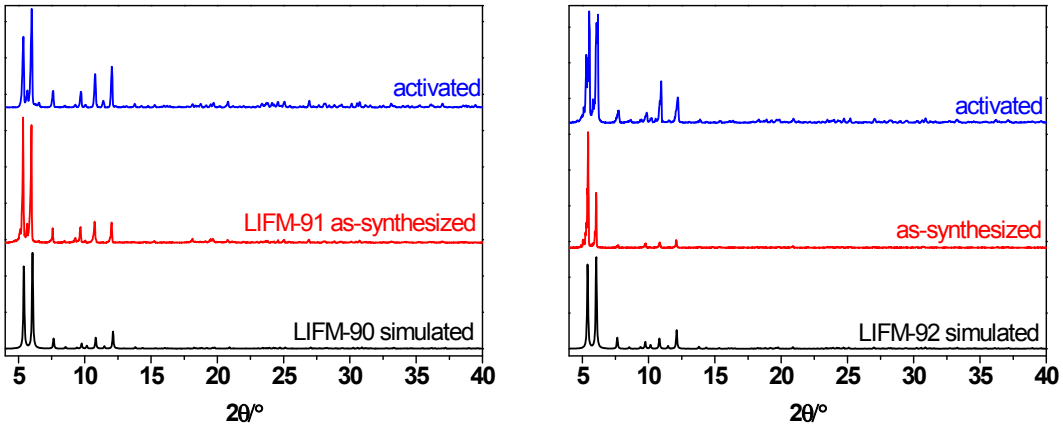

Fig. S4 PXRD patterns of LIFM-91 (left) and LIFM-92 (right).

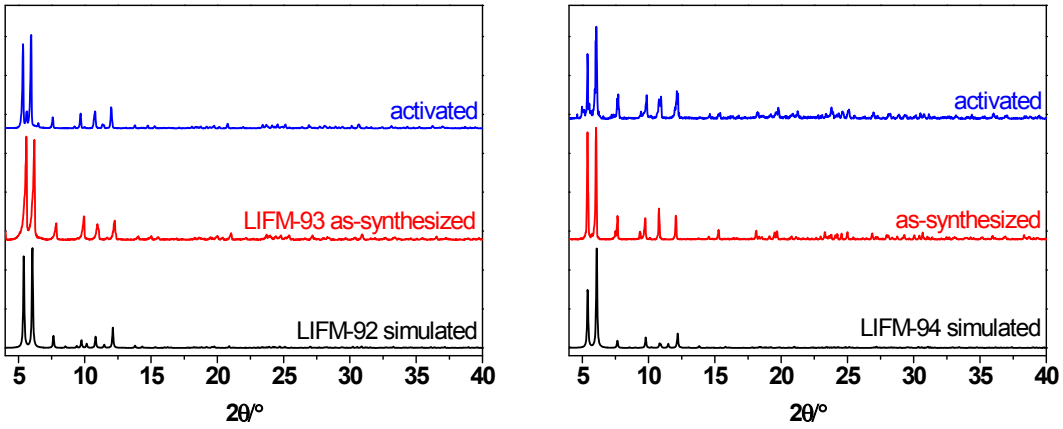

Fig. S5 PXRD patterns of LIFM-93 (left) and LIFM-94 (right).

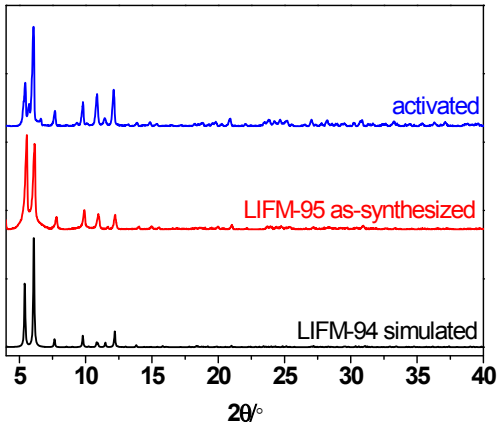

Fig. S6 PXRD patterns of LIFM-95.

S6. TGA

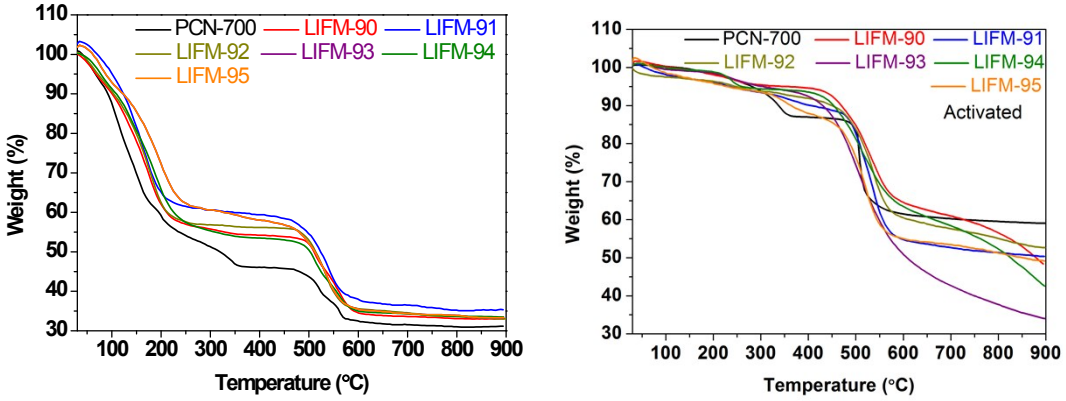

Fig. S7 The thermogravimetric analysis of as-synthesized (left) and activated (right) PCN-700 and LIFM-90—95 under N_2 atmosphere.

S6. Infrared Spectroscopy

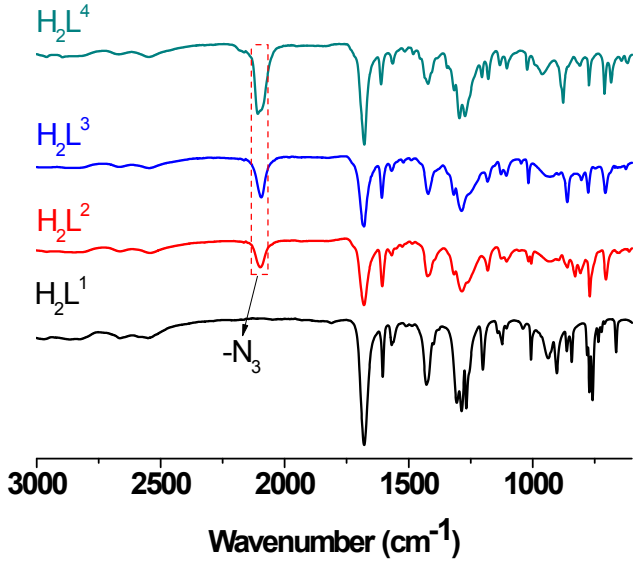

Fig. S8 Infrared spectra of H_2L^1, H_2L^2, H_2L^3 and H_2L^4.

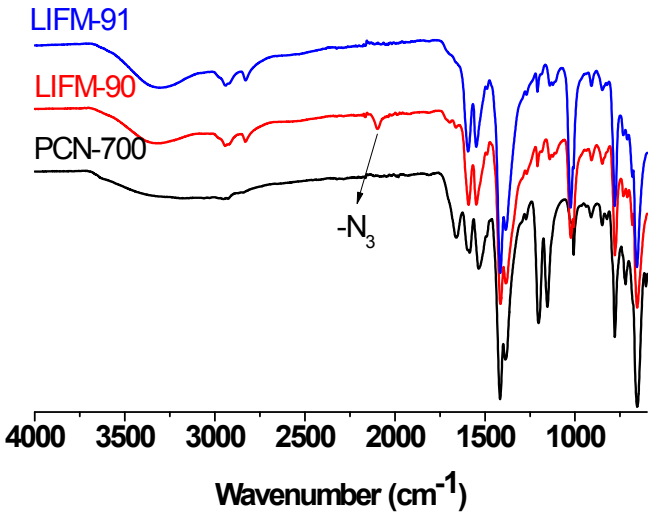

Fig. S9 Infrared spectra of PCN-700, LIFM-90 and LIFM-91.

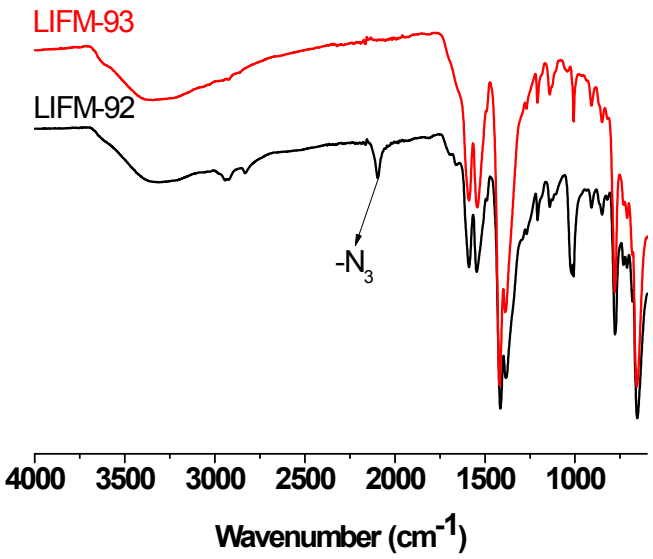

Fig. S10 Infrared spectra of LIFM-92 and LIFM-93.

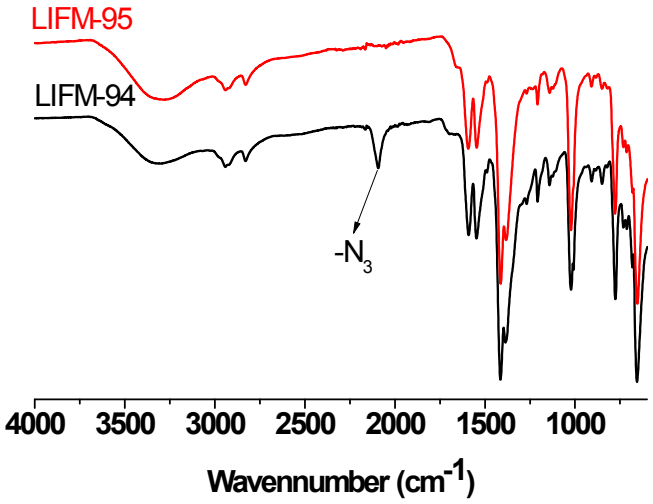

Fig. S11 Infrared spectra of LIFM-94 and LIFM-95.

S7. Porosity, Selectivity and Gas Adsorption Properties

PCN-700, LIFM-90, LIFM-91, LIFM-92, LIFM-93, LIFM-94 and LIFM-95 were subsequently washed with DMF and immersed in anhydrous methanol for 3 days, during which the solvent was decanted and freshly replenished three times a day. The samples were activated under vacuum at 100 ℃ for 12 hours. Gas sorption measurements were then conducted using a Quantachrome Autosorb-iQ2-MP gas adsorption analyzer.

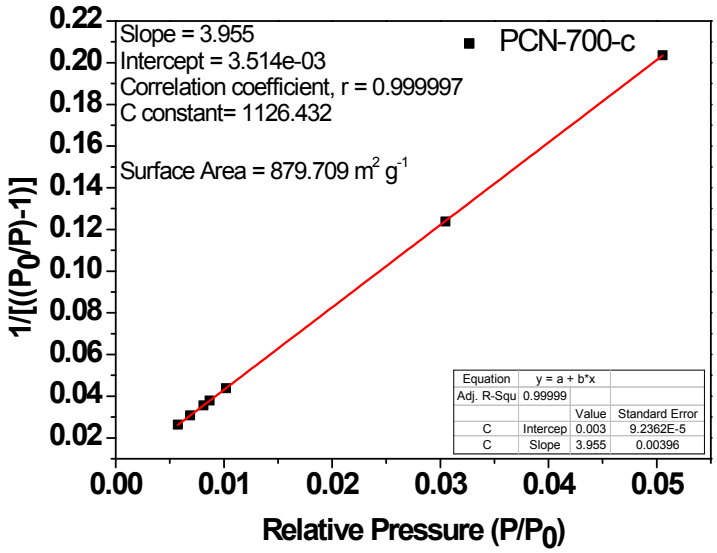

Fig. S12 Plot of the linear region on the N_2 isotherm of PCN-700-c for the BET equation.

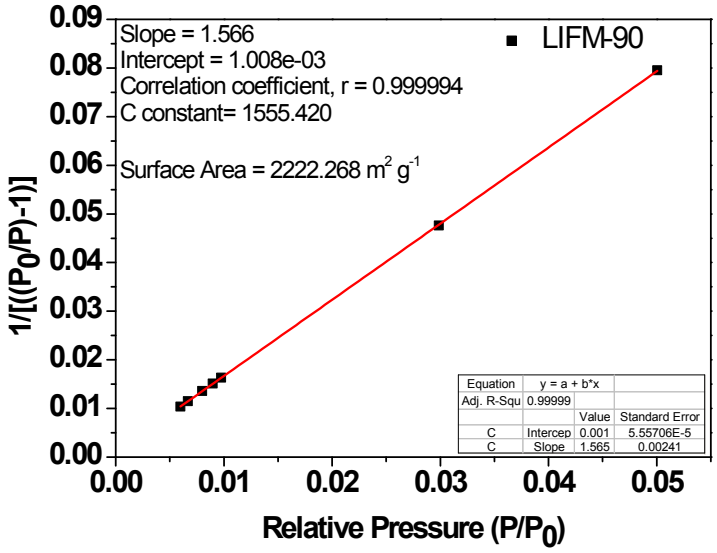

Fig. S13 Plot of the linear region on the N_2 isotherm of LIFM-90 for the BET equation.

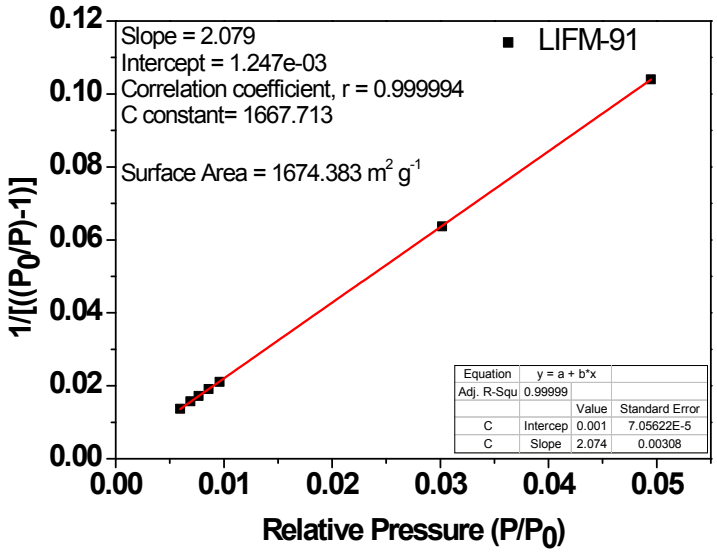

Fig. S14 Plot of the linear region on the N_2 isotherm of LIFM-91 for the BET equation.

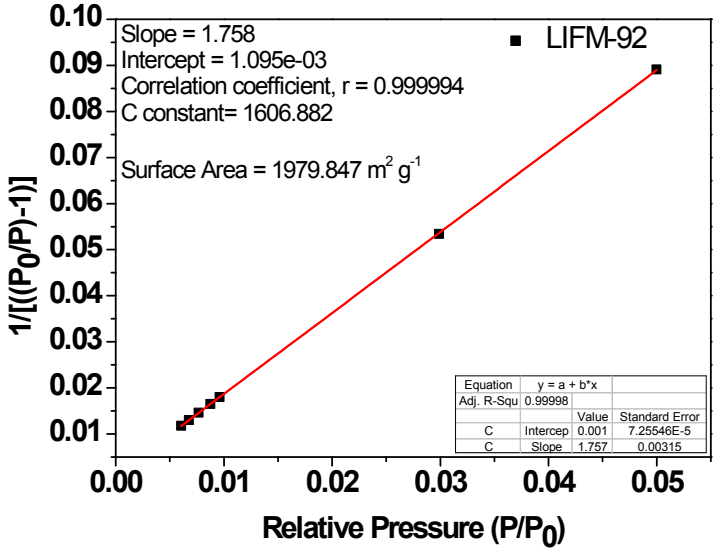

Fig. S15 Plot of the linear region on the N_2 isotherm of LIFM-92 for the BET equation.

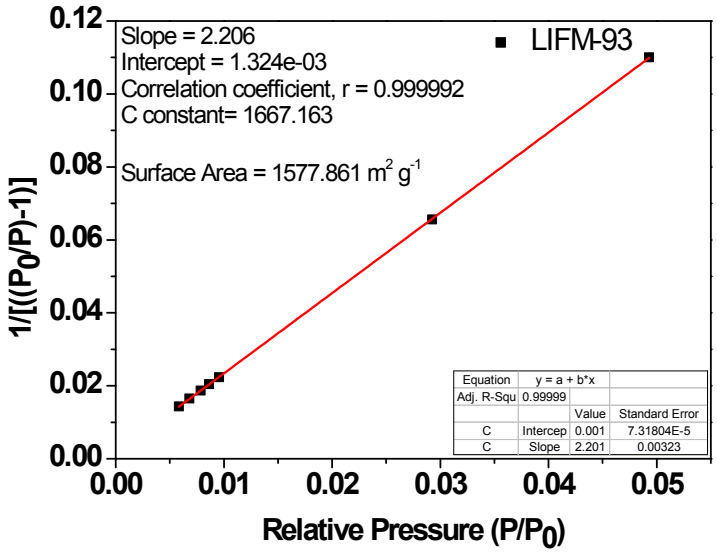

Fig. S16 Plot of the linear region on the N_2 isotherm of LIFM-93 for the BET equation.

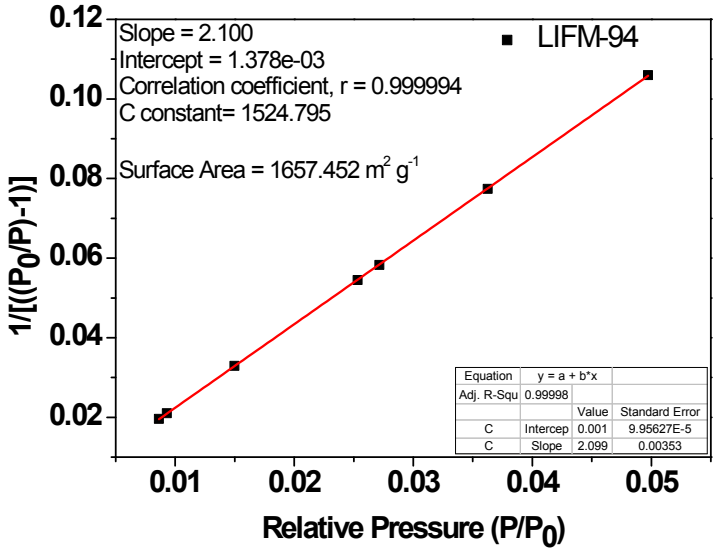

Fig. S17 Plot of the linear region on the N_2 isotherm of LIFM-94 for the BET equation.

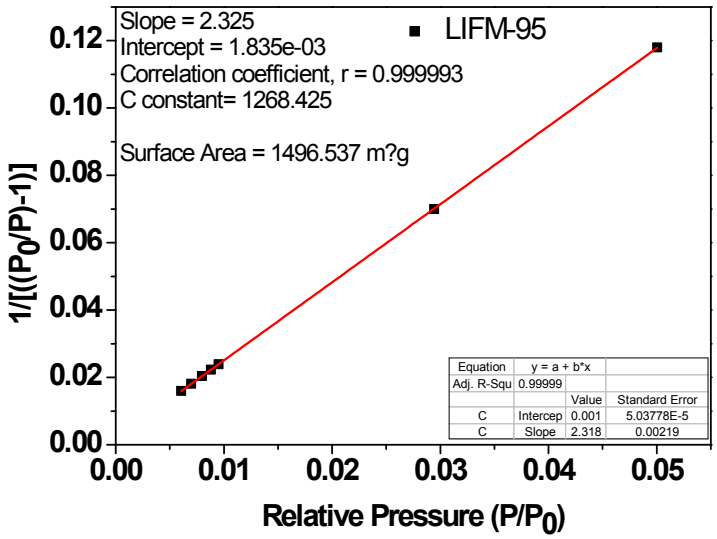

Fig. S18 Plot of the linear region on the N_2 isotherm of LIFM-95 for the BET equation.

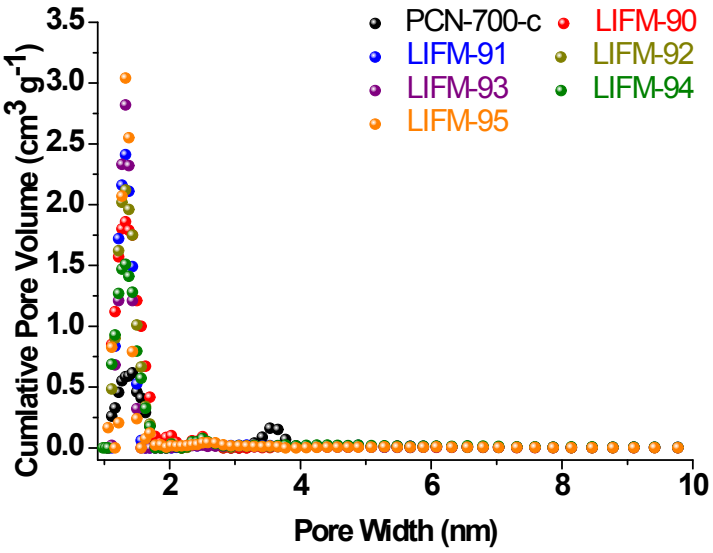

Fig. S19 Pore size distribution of PCN-700-c, LIFM-90, LIFM-91, LIFM-92, LIFM-93, LIFM-94 and LIFM-95 calculated from SF analysis.

Table S2 Summary of porosity parameters of PCN-700-c, LIFM-90—95.

Structure	S_{BET} (m^2/g)	Total Pore Volume (cc/g)	Pore Size by DFT (Å)

PCN-700-c	879	0.41	14.3
LIFM-90	2222	0.92	13.2
LIFM-91	1674	0.74	13.2
LIFM-92	2175	0.84	13.2
LIFM-93	1577	0.69	12.7
LIFM-94	1657	0.77	13.2
LIFM-95	1496	0.63	12.7

S8. H_2, R22, CO_2, CH_4, N_2 Sorption Isotherm

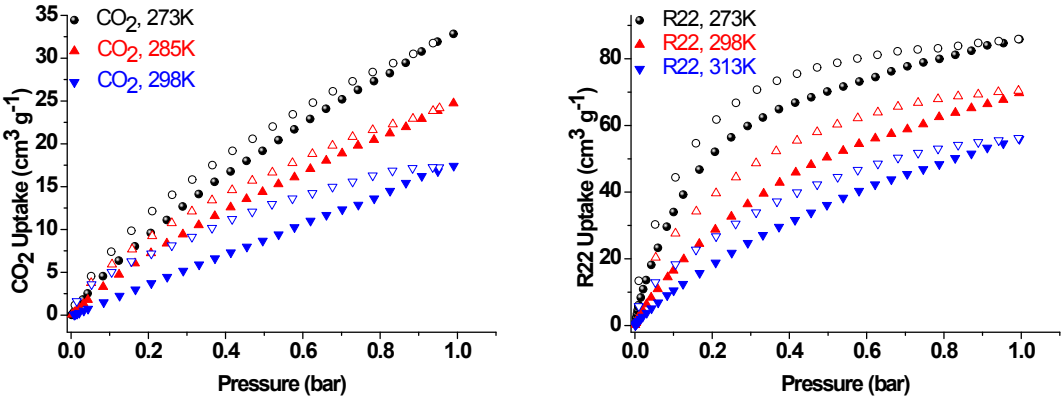

Fig. S20 CO_2 and R22 sorption isotherms of PCN-700-c at three different temperatures. Solid symbols: adsorption; open symbols: desorption.

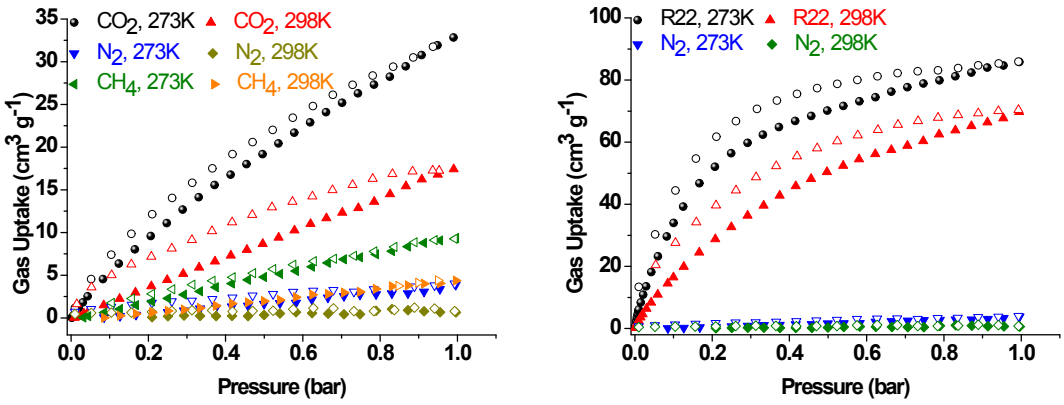

Fig. S21 CO_2, R22, N_2 and CH_4 sorption isotherms of PCN-700-c. Solid symbols: adsorption; open symbols: desorption.

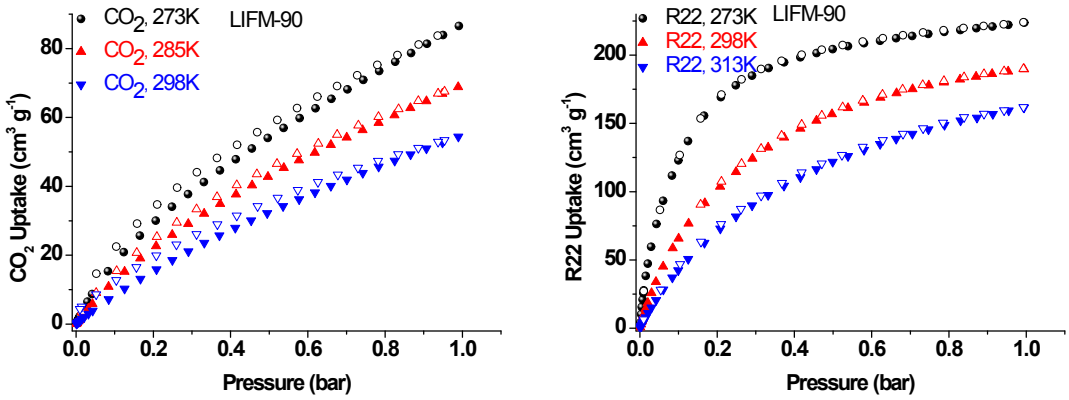

Fig. S22 CO_2 and R22 sorption isotherms of LIFM-90 at three different temperatures. Solid symbols: adsorption; open symbols: desorption.

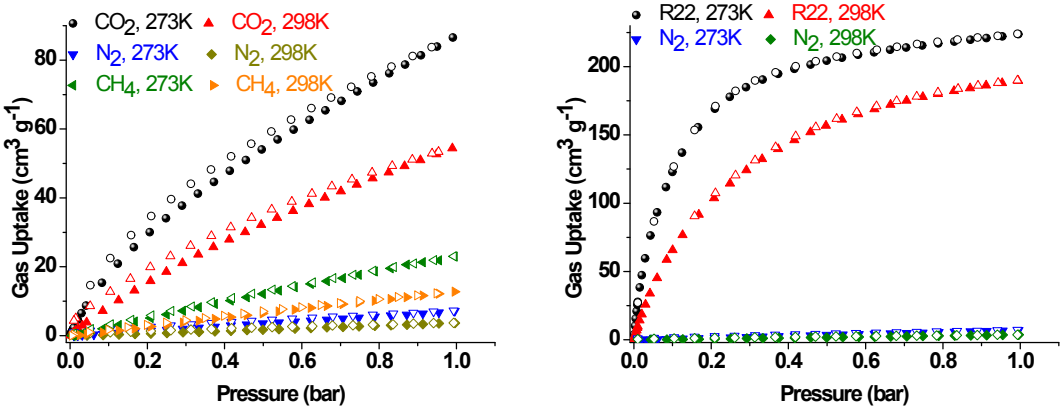

Fig. S23 CO_2, R22, N_2 and CH_4 sorption isotherms of LIFM-90. Solid symbols: adsorption; open symbols: desorption.

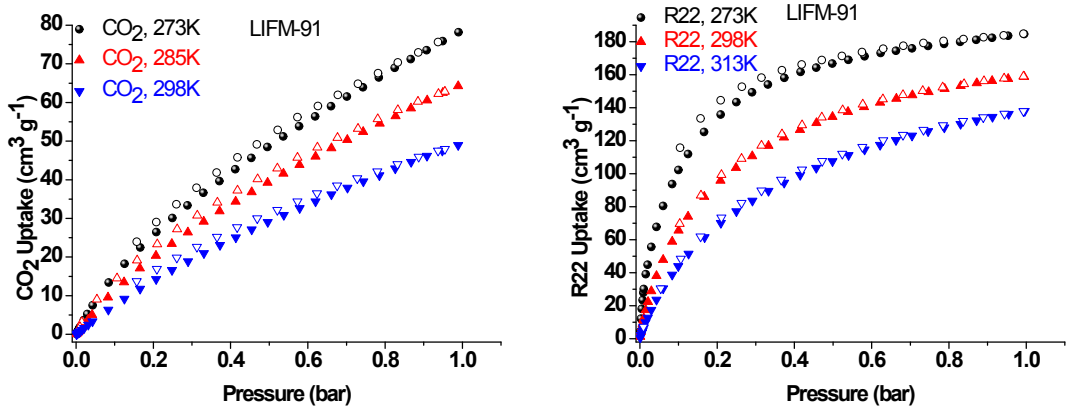

Fig. S24 CO_2 and R22 sorption isotherms of LIFM-91 at three different temperatures. Solid symbols: adsorption; open symbols: desorption.

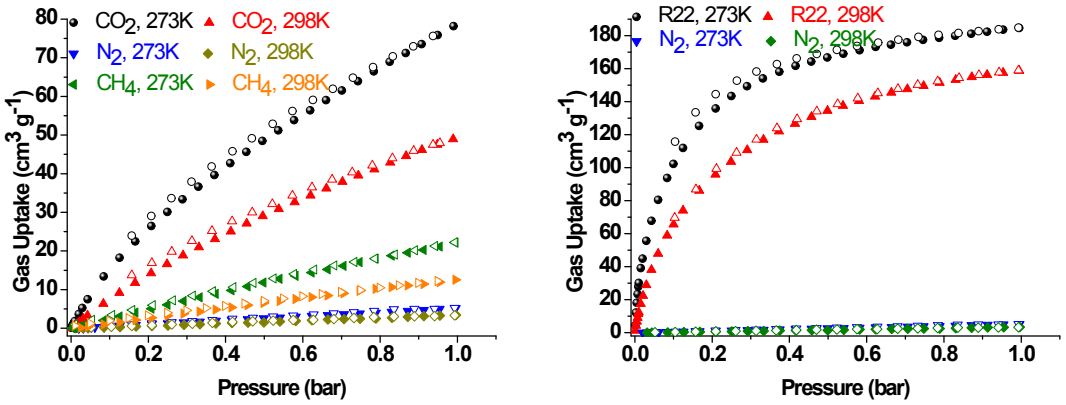

Fig. S25 CO_2, R22, N_2 and CH_4 sorption isotherms of LIFM-91. Solid symbols: adsorption; open symbols: desorption.

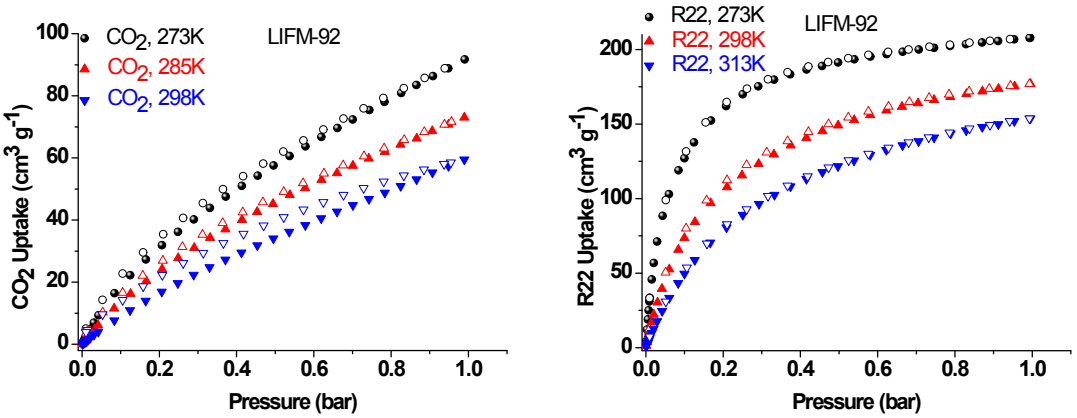

Fig. S26 CO_2 and R22 sorption isotherms of LIFM-92 at three different temperatures. Solid symbols: adsorption; open symbols: desorption.

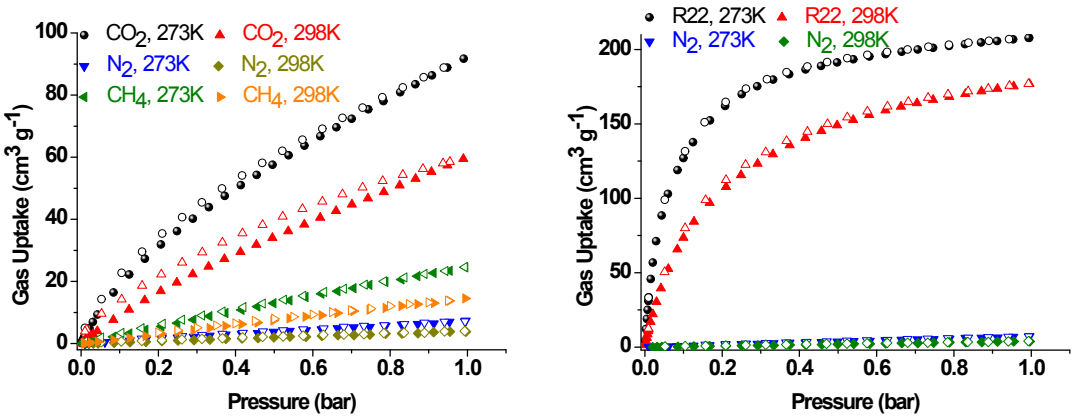

Fig. S27 CO_2, R22, N_2 and CH_4 sorption isotherms of LIFM-92. Solid symbols: adsorption; open symbols: desorption.

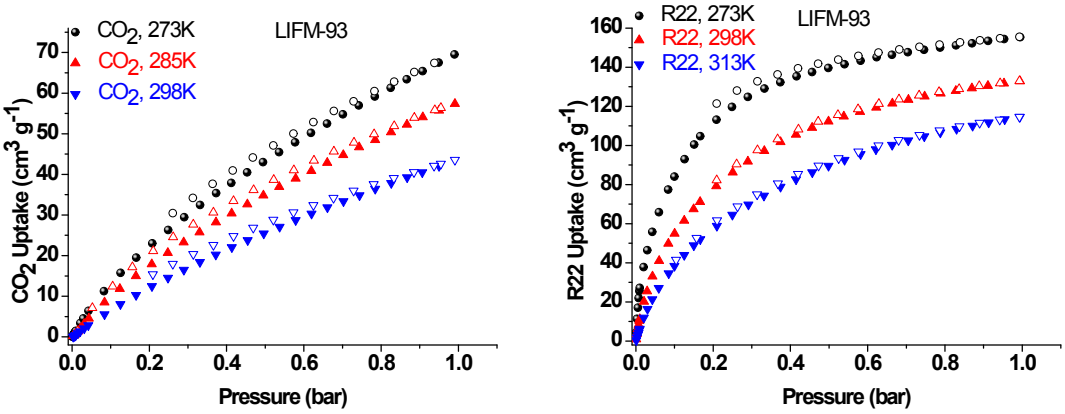

Fig. S28 CO_2 and R22 sorption isotherms of LIFM-93 at three different temperatures. Solid symbols: adsorption; open symbols: desorption.

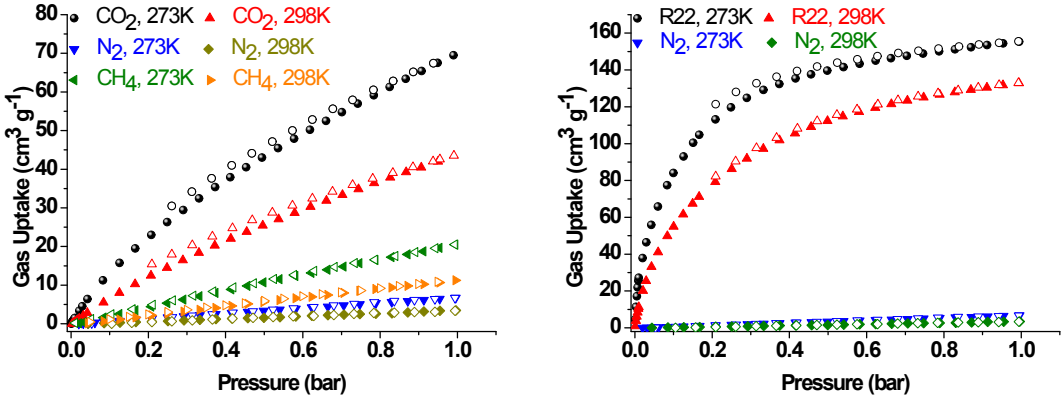

Fig. S29 CO_2, R22, N_2 and CH_4 sorption isotherms of LIFM-93. Solid symbols: adsorption; open symbols: desorption.

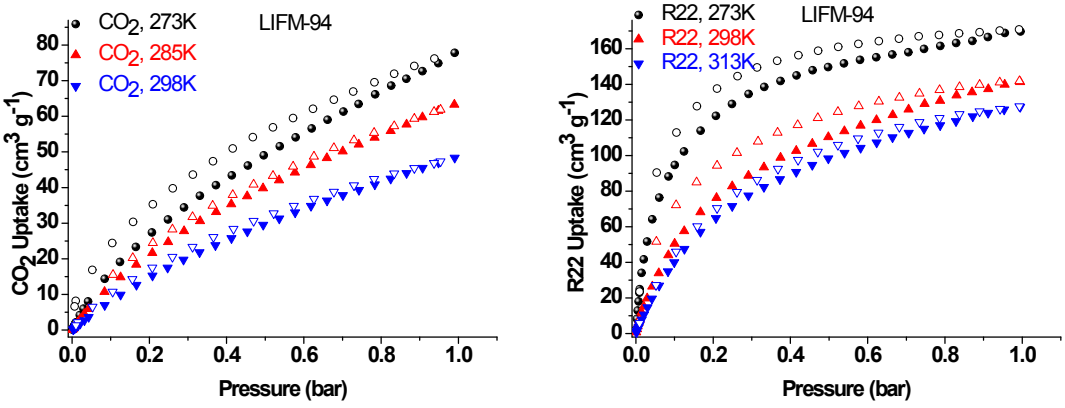

Fig. S30 CO_2 and R22 sorption isotherms of LIFM-94 at three different temperatures. Solid symbols: adsorption; open symbols: desorption.

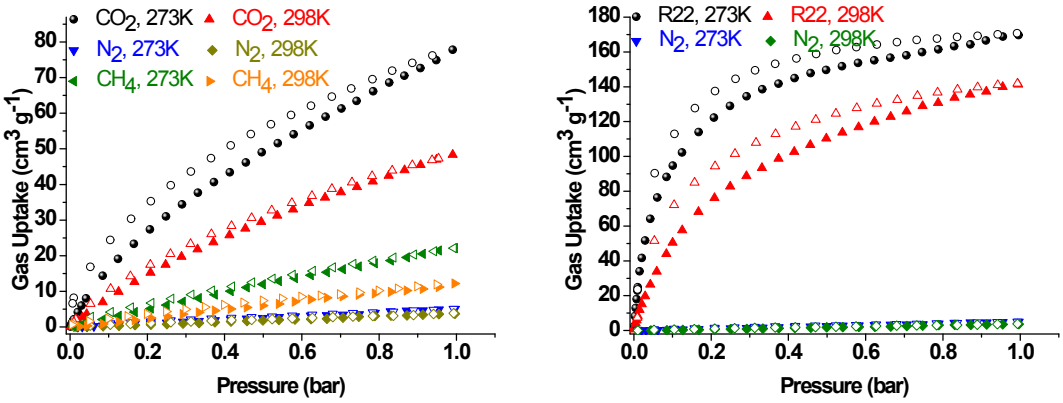

Fig. S31 CO_2, R22, N_2 and CH_4 sorption isotherms of LIFM-94. Solid symbols: adsorption; open symbols: desorption.

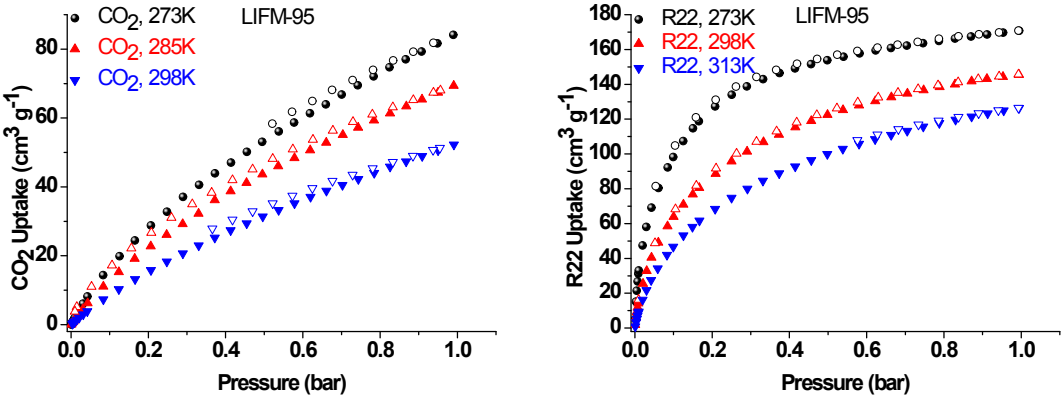

Fig. S32 CO_2 and R22 sorption isotherms of LIFM-95 at three different temperatures. Solid symbols: adsorption; open symbols: desorption.

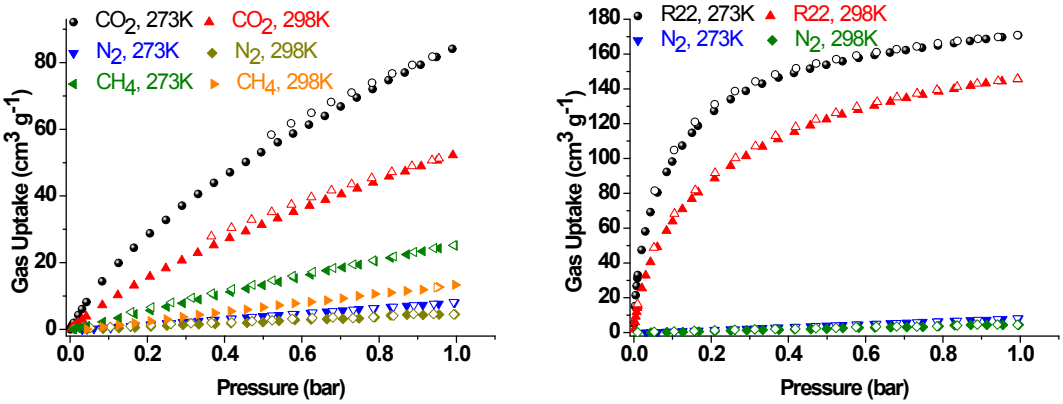

Fig. S33 CO_2, R22, N_2 and CH_4 sorption isotherms of LIFM-95. Solid symbols: adsorption; open symbols: desorption.

S9. Calculations of Adsorption Isosteric Heats:

The isosteric heats of R22 and CO_2 adsorption for PCN-700-c, LIFM-90—95 were calculated from the sorption data measured at three different temperatures by the virial fitting method, respectively. A virial-type expression (eq. 1) which is composed of parameters a_i and b_i is used. In eq. 1, P is the pressure in torr, N is the adsorbed amount in mmol·g^{-1}, T is the temperature in Kelvin, a_i and b_i are the virial coefficients which are independent of temperature, and m and n are the numbers of coefficients required to adequately describe the isotherms.

$$\ln P = \ln N + \frac{1}{T}\sum_{i=0}^{m} a_i N^i + \sum_{i=0}^{n} b_i N^i \qquad \text{eq. 1}$$

The values of the virial coefficients a_0 through a_m were then applied to calculate the isosteric heat of adsorption (eq 2). In eq. 2, Q_{st} is the coverage-dependentisosteric heat of adsorption and R is the universal gas constant.[6]

$$Q_{st} = -R\sum_{i=0}^{m} a_i N^i \qquad \text{eq. 2}$$

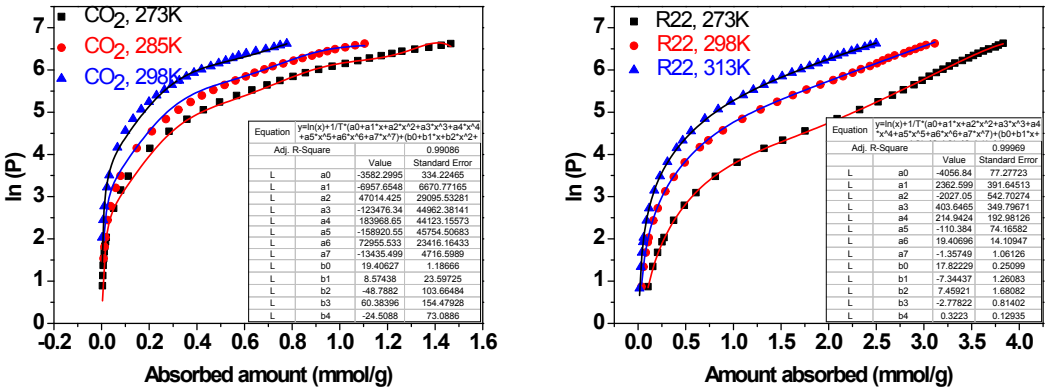

Fig. S34 CO_2 and R22 fitting (lines) of the adsorption isotherms (points) of PCN-700-c at different temperatures.

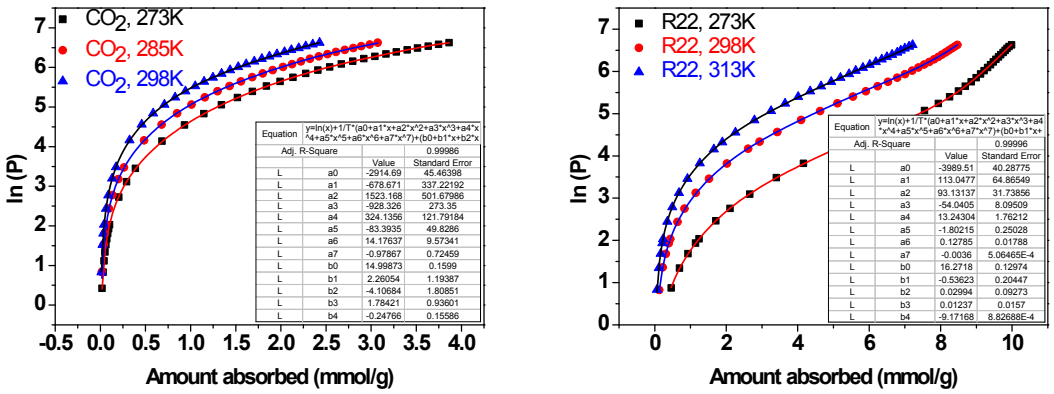

Fig. S35 CO_2 and R22 fitting (lines) of the adsorption isotherms (points) of LIFM-90 at different temperatures.

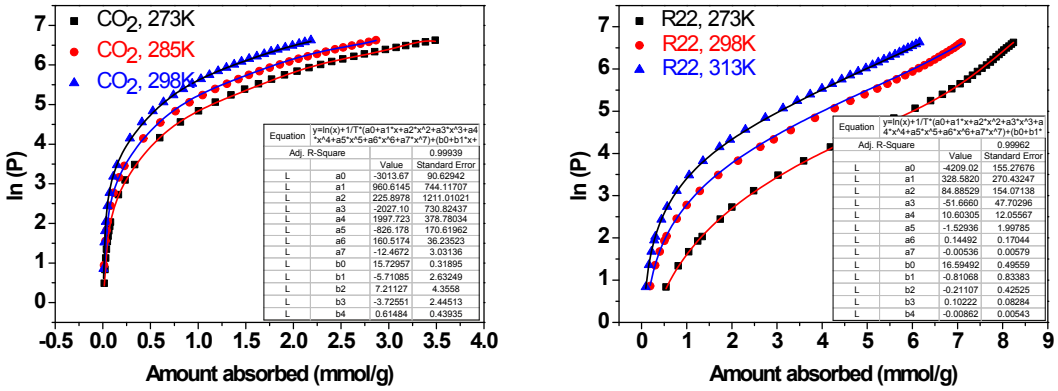

Fig. S36 CO_2 and R22 fitting (lines) of the adsorption isotherms (points) of LIFM-91 at different temperatures.

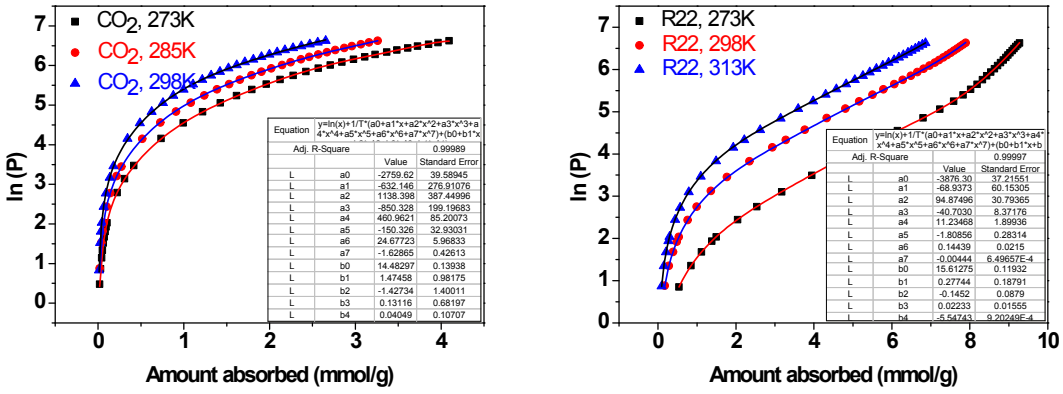

Fig. S37 CO_2 and R22 fitting (lines) of the adsorption isotherms (points) of LIFM-92 at different temperatures.

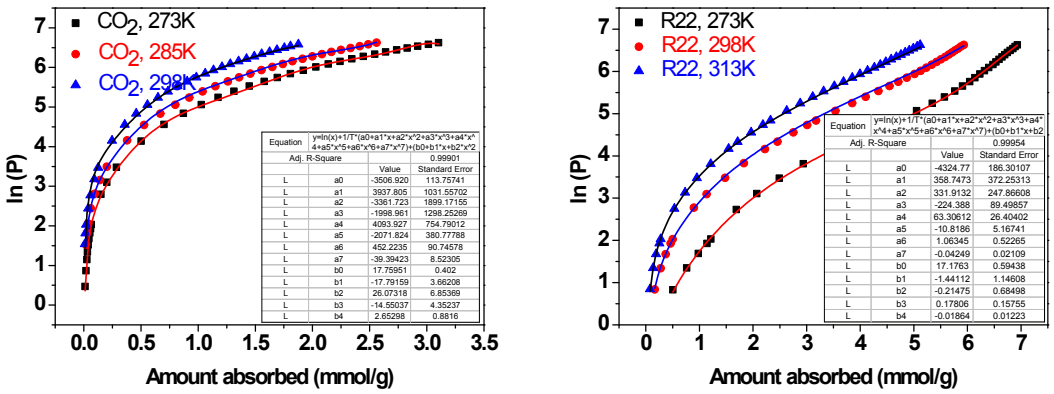

Fig. S38 CO_2 and R22 fitting (lines) of the adsorption isotherms (points) of LIFM-93 at different temperatures.

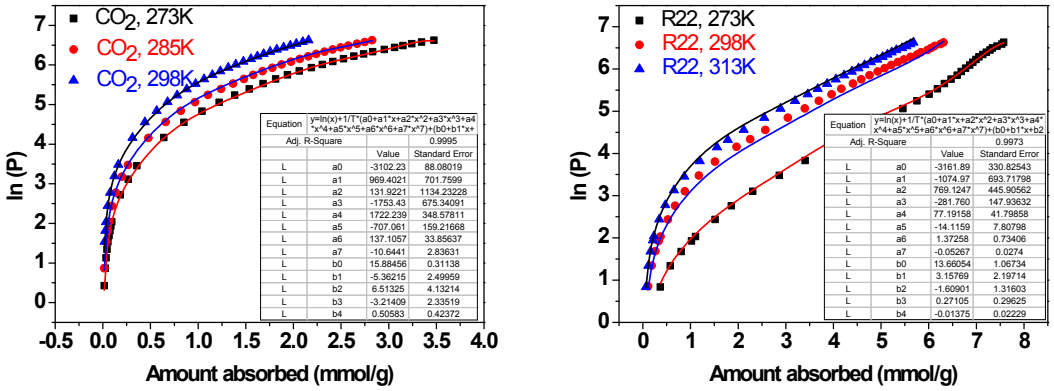

Fig. S39 CO_2 and R22 fitting (lines) of the adsorption isotherms (points) of LIFM-94 at different temperatures.

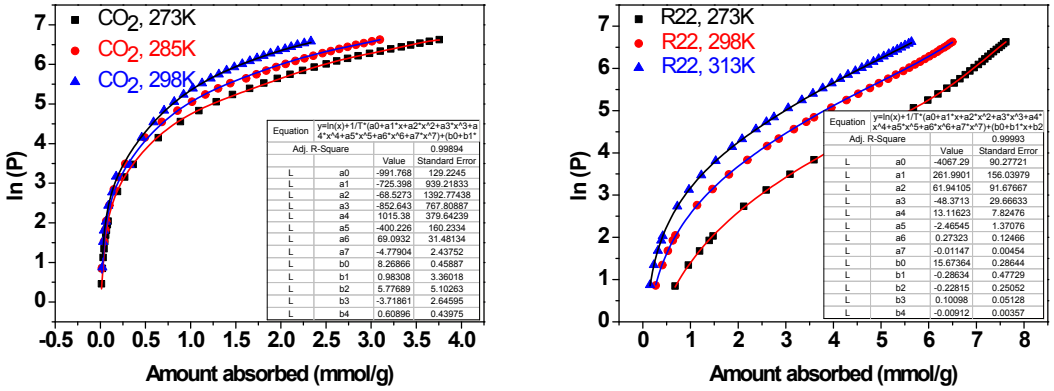

Fig. S40 CO_2 and R22 fitting (lines) of the adsorption isotherms (points) of LIFM-95 at different temperatures.

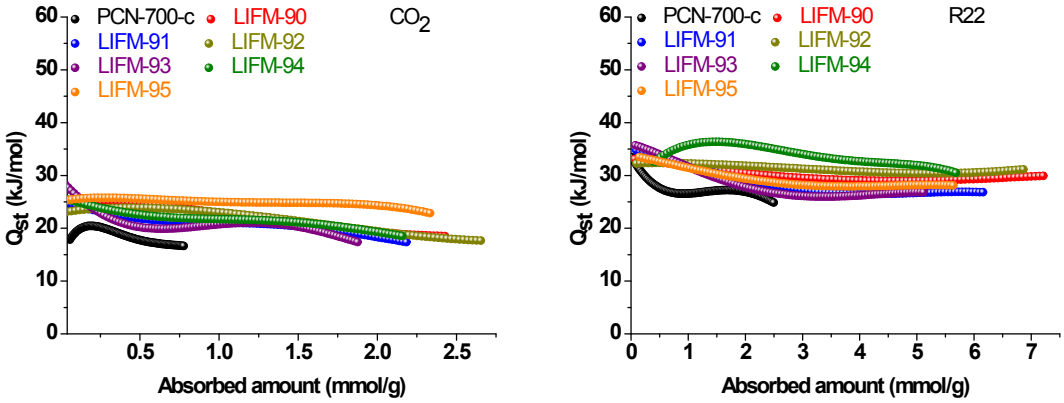

Fig. S41 CO_2 (left) and R22 (right) isosteric heat of adsorption in PCN-700-c, LIFM-90, LIFM-91, LIFM-92, LIFM-93, LIFM-94 and LIFM-95 as a function of surface coverage.

S10. R22/N_2, CO_2/N_2 and CO_2/CH_4 Selectivity Calculation via IAST

The experimental isotherm data for pure CO_2 and R22 (measured at 273 K and 298 K) were fitted using a Langmuir Freundlich (LF) model:

$$q = \frac{a * b * p^{1/n}}{1 + b * p^{1/n}} \quad \text{eq. 3}$$

Where q and p are adsorbed amounts and pressure of component i, respectively.

The adsorption selectivities for binary mixtures of R22/N_2, CO_2/N_2 and CO_2/CH_4 defined by

$$S_{i/j} = \frac{x_i}{x_j} * \frac{y_j}{yi} \quad \text{eq. 4}$$

were calculated using the Ideal Adsorption Solution Theory (IAST) of Myers and Prausnitz.[7] Where x_i is the mole fraction of component i in the adsorbed phase and y_i is the mole fraction of component i in the bulk.

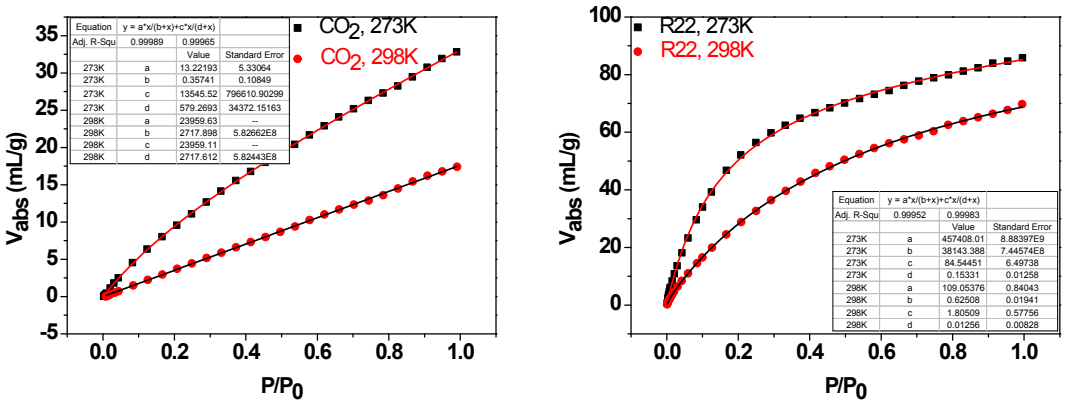

Fig. S42 CO_2, R22 adsorption isotherms of PCN-700-c with fitting by LF model.

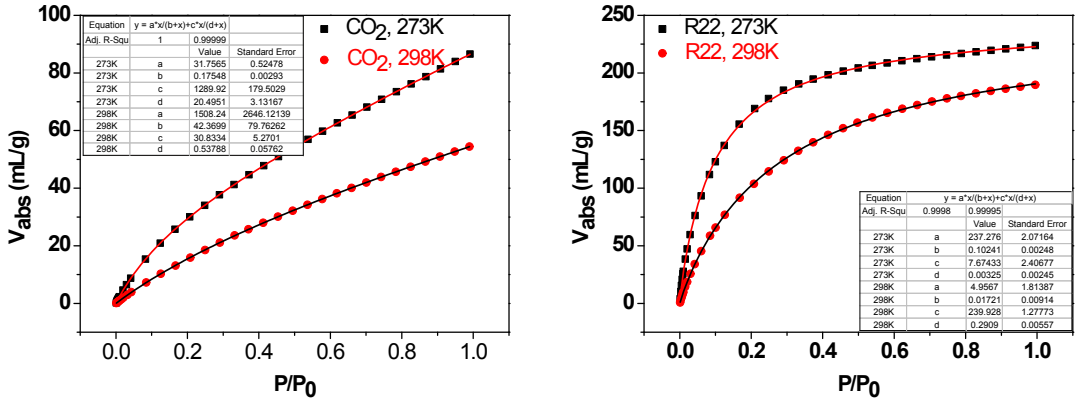

Fig. S43 CO_2, R22 adsorption isotherms of LIFM-90 with fitting by LF model.

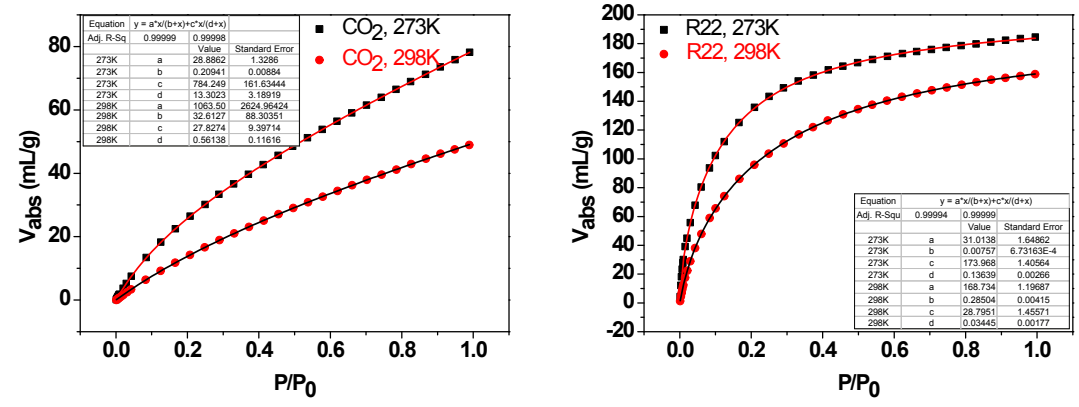

Fig. S44 CO_2, R22 adsorption isotherms of LIFM-91 with fitting by LF model.

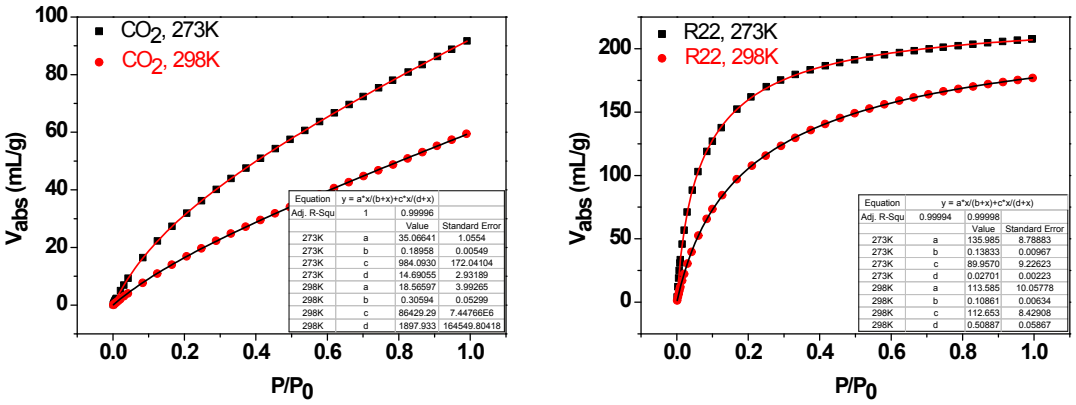

Fig. S45 CO_2, R22 adsorption isotherms of LIFM-92 with fitting by LF model.

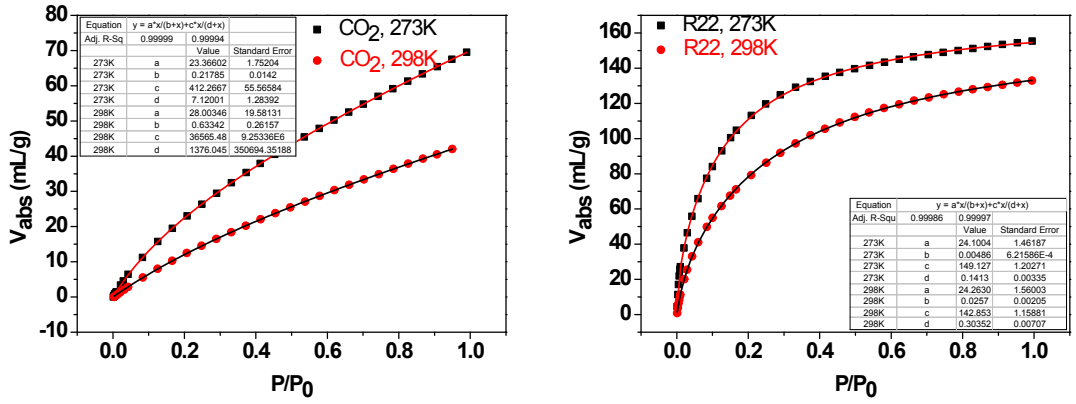

Fig. S46 CO_2, R22 adsorption isotherms of LIFM-93 with fitting by LF model.

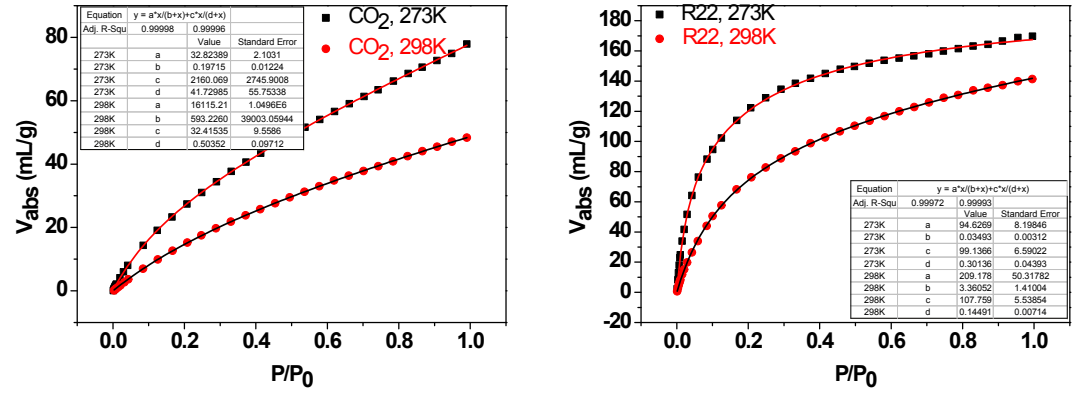

Fig. S47 CO_2, R22 adsorption isotherms of LIFM-94 with fitting by LF model.

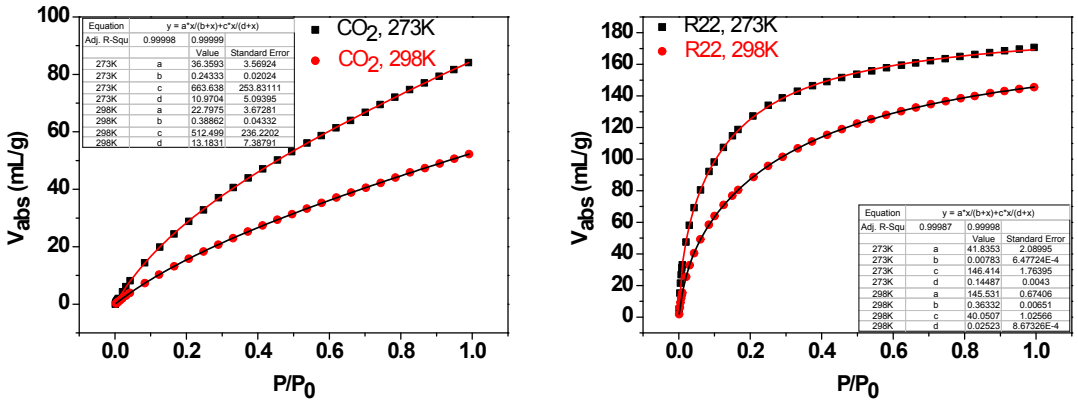

Fig. S48 CO_2, R22 adsorption isotherms of LIFM-95 with fitting by LF model.

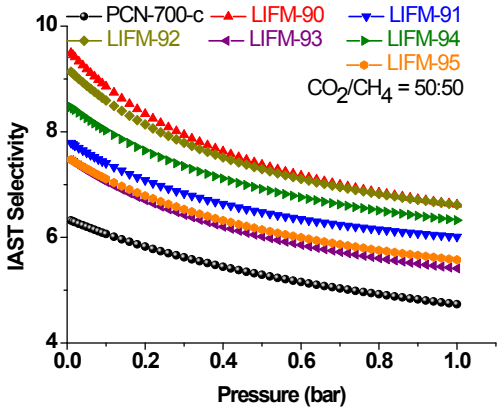

Fig. S49 IAST calculative selectivity of CO_2/CH_4 on all the MOFs at 273 K.

S11. ^{1}H NMR Spectroscopy

For ^{1}H NMR analysis of LIFM-90, LIFM-92 and LIFM-94, the activated samples (around 10 mg) were digested with sonication in 490 μL DMSO-d^6 and 10 μL of 40% HF.

^{1}H NMR spectra for LIFM-90, LIFM-92 and LIFM-94 are presented below.

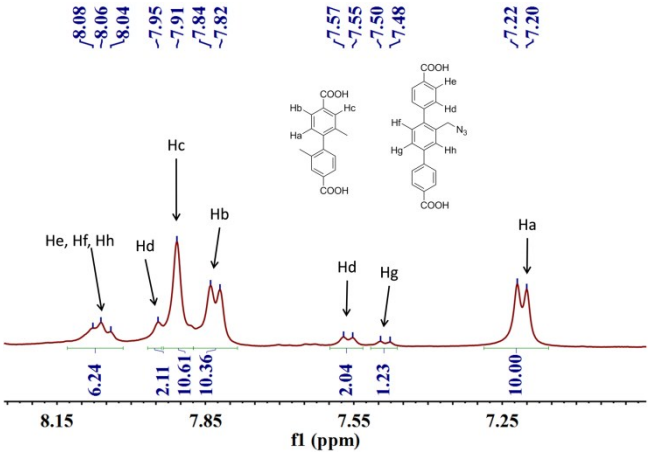

Fig. S50 [1]H NMR spectroscopy of digested LIFM-90.

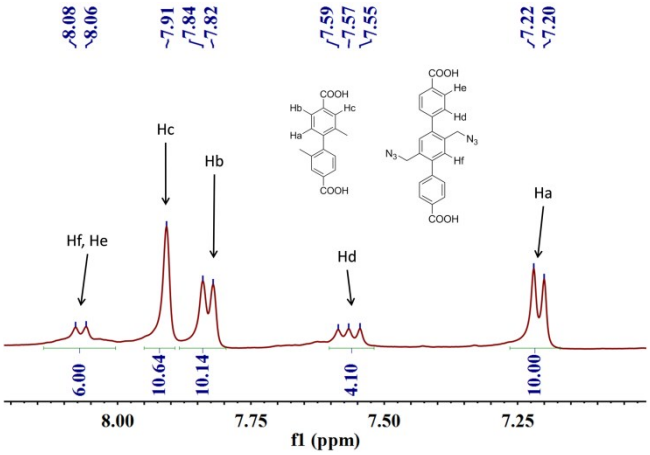

Fig. S51 [1]H NMR spectroscopy of digested LIFM-92.

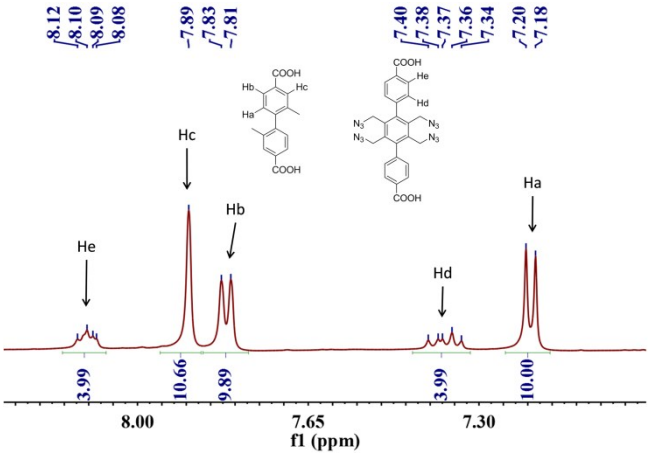

Fig. S52 [1]H NMR spectroscopy of digested LIFM-94.

Table S3 Comparison of spacer ratios from single crystal structure and from [1]H NMR of digested samples.

MOF	Spacer ratios from single crystal structure	Spacer ratios from ^{1}H NMR and ^{19}F NMR of digested samples[a]
LIFM-90	L^1:L^2 = 5:1	L^1:L^2 = 10.36/2:(2.04/2) = 5.08:1
LIFM-92	L^1:L^3 = 5:1	L^1:L^3 =10.14/2: (4.10/4) = 4.95:1
LIFM-94	L^1:L^4 = 5:1	L^1:L^4 = 9.89/2: (3.99/4) = 4.96:1

[a] Based on integral area of corresponding H peaks.

S16 Regeneration of LIFM-92 and LIFM-93

LIFM-92 and LIFM-93 are selected as representative to demonstrate that these MOFs can be regenerated under mild conditions. The samples of LIFM-92 and LIFM-93 are vacuumed at room temperature for regeneration after each run of gas adsorption. The repeated CO_2 and R22 adsorptions for these two MOFs are plotted below.

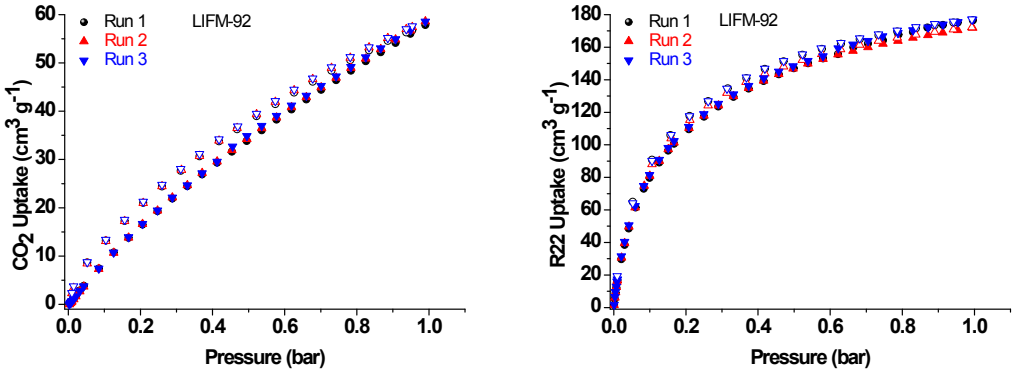

Fig. S53 Repeated CO_2 and R22 sorption isotherms of LIFM-92 at 298K after regeneration. Solid symbols: adsorption; open symbols: desorption.

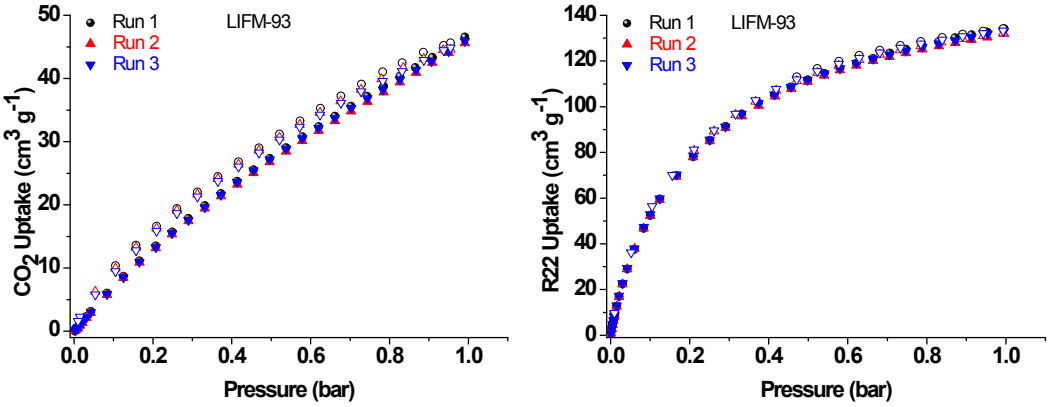

Fig. S54 Repeated CO_2 and R22 sorption isotherms of LIFM-93 at 298K after regeneration. Solid symbols: adsorption; open symbols: desorption.

S17 References

1 S. Yuan, W. Lu, Y.-P. Chen, Q. Zhang, T.-F. Liu, D. Feng, X. Wang, J. Qin and H.-C. Zhou, *J. Am. Chem. Soc.*, 2015, **137**, 3177.

2 H.-L. Jiang, D. Feng, T.-F. Liu, J.-R. Li and H.-C. Zhou, *J. Am. Chem. Soc.*, 2012, **134**, 14690.

3 P. V. Dau, S. M. Cohen, *Inorg. Chem.* **2015**, *54*, 3134.

4 N. Ko, J. Hong, S. Sung, K. E. Cordova, H. J. Park, J. K. Yang, J. Kim, *Dalton. Trans.* **2015**, *44*, 2047.

5 Accelrys *Materials Studio Release Motes, Release 6.1.0*; Accelrys Software, Inc. , San Diego, 2012.

6 L. Czepirski, J. J., *Chem. Eng. Sci.* **1989**, *44*, 797.

7 Myers, A. L.; Prausnitz *J. M. AIChE.* **1965**, *11*, 121.